SUPPLEMENTARY MATERIAL

α-Glucosidase inhibitory, antibacterial, and antioxidant activities of natural substances from the wood of *Derris reticulata* Craib

Papawarin Issarachot[a], Warissara Sangkaew[a], Wipawadee Sianglum[b], Dennapa Saeloh[c,d], Surasak Limsuwan[a,c], Supayang Piyawan Voravuthikunchai[b,c], and Nantiya Joycharat[a,c*]

[a]*Faculty of Traditional Thai Medicine, Prince of Songkla University, Songkhla 90112, Thailand*

[b]*Department of Microbiology, Faculty of Science, Prince of Songkla University, Songkhla 90112, Thailand*

[c]*Excellent Research Laboratory on Natural Products, Faculty of Science and Natural Product Research Center of Excellence, Prince of Songkla University, Songkhla 90112, Thailand*

[d]*Faculty of Medical Technology, Prince of Songkla University, Songkhla 90112, Thailand*

[*]Corresponding author: Nantiya Joycharat. Faculty of Traditional Thai Medicine, Prince of Songkla University, Hat Yai, Songkhla 90112, Thailand. Tel.: +66-74-282722, Fax: +66-74-282709, E-mail: nantiya.j@psu.ac.th

ABSTRACT

Derris reticulata (Leguminosae-Papilionoideae) has been used for the treatment of diabetes in Thai folk remedies. The phytochemical investigation of the wood of *D. reticulata* revealed the isolation of two new pyranoflavanones, 4′-methoxydereticulatin (**1**) and 2′′′-hydroxy,3′′′-ethoxylupinifolin (**2**), along with five known compounds namely lupinifolin (**3**), 2′′′,3′′′-dihydroxylupinifolin (**4**), genistein (**5**), lupeol (**6**), and β-sitosterol (**7**). Compounds **1**-**4** were selected for antibacterial assay using broth microdilution method, and displayed good activity against four out of five tested pathogenic bacterial strains, with MIC values ranging from 0.78 to 128 μg/mL. The result from spectrophotometric assay of α-glucosidase inhibition showed that **5** exhibited promising α-glucosidase inhibitory activity, compared with the positive control acarbose. Additionally, it was found that compounds **4** and **5** showed moderate DPPH and NO radicals scavenging activity. Modeling studies were also performed to suggest the interaction modes of compounds **3**-**5** in the α-glucosidase enzyme active site.

Keywords: α-glucosidase; diabetes; flavanone; molecular docking; natural products

Experimental

General

The following devices and chemicals were used: 1D- and 2D-NMR, FTNMR Bruker Advance 500 MHz (Bruker Corporation, New Orleans, LA); HRESIMS, Bruker Daltonics micrOTOF (Bruker Corporation, New Orleans, LA); Column chromatography (CC) was performed using silica gel (70–230 mesh, Merck, New York, USA), and Sephadex LH-20 (20–100 mm, Sigma, St. Louis, MO). Thin-layer chromatography (TLC) was performed on precoated sheets of silica gel 60 F_{254} (20 × 20 cm^2, 0.25 mm, Merck, New York, USA). Fractions and compounds were monitored by TLC sprayed with an anisaldehyde-sulfuric acid solution. All solvents were of laboratory reagent grade and were purchased from commercial sources.

Plant material

The stem wood of *D. reticulata* was purchased from central part of Thailand in October 2017. The identification of plant material was done by Assoc. Prof. Dr. Oratai Neamsuvan of the Faculty of Traditional Thai Medicine, Prince of Songkla University, where a voucher specimen (NJ-C1017) was deposited.

Isolation and purification

The wood of *D. reticulata* (2 kg) was dried, ground, and macerated with ethanol (EtOH) at room temperature, filtered, and concentrated to give a residue of EtOH extract (7.09%). The EtOH extract was partitioned to produce *n*-hexane, dichloromethane (CH_2Cl_2), and *n*-butanol (*n*-BuOH) fractions. The yields of *n*-hexane, CH_2Cl_2, and *n*-BuOH fractions were 3.21%, 0.32%, and 3.55%, respectively.

The dichloromethane fraction (10 g) was applied to silica gel CC using gradient elution with acetone–hexane, and finally washed down with MeOH. The fractions showing similar TLC profiles were then combined and numbered (ID–VD). Fraction IID (235 mg) was recrystallized with 20% acetone in hexane to give **3** (208 mg). Fraction IVD (366.4 mg) was further subjected to Sephadex LH-20 column eluted with $CHCl_3$: MeOH (1:1) to yield subfractions I–VII. Subfraction III (215.1 mg) was further purified on repeated silica gel chromatography ((i) CC gradient acetone–hexane and (ii) CC acetone–$CHCl_3$) and Sephadex LH-20 column eluted with $CHCl_3$: MeOH (1:1) to yield compounds **1** (7.3 mg), **2** (2.0 mg),

and **4** (10.6 mg). Subfraction VI (15.1 mg) was further recrystallized with 40% acetone in hexane to give **5** (14.1 mg). In the present work, additional quantity of **3**, along with lupeol (**6**) and β-sitosterol (**7**) was obtained from the *n*-hexane fraction of *D. reticulata* using column chromatography described previously (Joycharat et al. 2016).

4′-methoxydereticulatin (**1**). Yellow-orange amorphous solid; IR ν_{max} ($CHCl_3$) cm^{-1}: 3360, 3192, 2921, 2850, 1636, 1515, 1464, 1376, 1247, 1021, 835 (Figure S1); ^{1}H-NMR, ^{13}C-NMR, HMQC and HMBC (MeOH-d_4): see Table S1, Figures S2-S5; HRESIMS *m/z* 437.1967 $[M+H]^+$ (calcd. for $C_{26}H_{28}O_6$: 437.1964) (Figure S6).

2′′′-hydroxy,3′′′-ethoxylupinifolin (**2**). Pale yellow amorphous solid; IR ν_{max} ($CHCl_3$) cm^{-1} : 3359, 3194, 2922, 2852, 1632, 1518, 1462, 1377, 1162, 1125, 834 (Figure S5); ^{1}H-NMR, ^{13}C-NMR, HMQC and HMBC ($CDCl_3$): see Table S2, Figures S7-S11; HRESIMS *m/z* 469.2234 $[M+H]^+$ (calcd. for $C_{27}H_{32}O_7$: 469.2226) (Figure S12).

Antibacterial assay

Antibacterial activity of compounds isolated from *D. reticulata* against five bacteria pathogens including *Staphylococcus aureus*, *Staphylococcus epidermidis*, *Bacillus cereus*, *Streptococcus sobrinus*, and *Streptococcus mutans* was determined using broth microdilution method, reported previously (Joycharat et al. 2013; 2016). The culture and incubation conditions for all tested bacteria were based on standard protocols. Chlorhexidine and penicillin G were included as the positive controls. DMSO was used as a negative control. The results were recorded as the minimum inhibitory concentration (MIC) values.

Alpha-glucosidase activity assay

The *α*-glucosidase inhibitory activity of the isolated compounds from *D. reticulata* was carried out as described previously (Joycharat et al. 2018). The absorbance was measured spectrophotometrically at 405 nm using a microplate reader. Acarbose was used as a positive control, whereas DMSO (5%) was used as a negative control. The results were expressed as the percentage inhibition values and as IC_{50} values.

DPPH radical scavenging assay

The DPPH radical scavenging activity of the isolated compounds from *D. reticulata* was assessed using the method mentioned before (Bakastae et al. 2018). The reaction mixtures containing a 20 μL aliquot of tested agents (0.24 to 250 μg/mL) and a 180 μL of DPPH

solution(0.1 mM) were incubated for 30 min. The absorbance was measured at 515 nm in a microplate reader. Ascorbic acid was used as a reference standard. The results were recorded as percentage inhibition values and as IC_{50} values.

NO radical scavenging assay

Nitric oxide radical scavenging activity of the isolated compounds from *D. reticulata* was measured using the method reported previously with some modification (Green et al. 1982). The reaction mixtures containing a 80 μL aliquot of tested agents (0.49 to 500 μg/mL) and a 40 μL of sodium nitroprusside solution (25 mM) were incubated for 2.5 h. After the incubation period, a sulfanilamide solution (40 μL) and naphthylethylenediamine (40 μL) were added to the mixture. The absorbance was measured at 546 nm in a microplate reader. Catechin was used as a reference standard. The results were performed as percentage inhibition values and as IC_{50} values.

Molecular docking study in α-glucosidase inhibition

A crystal structure of *Saccharomyces cerevisiae* α-glucosidase, (PDB entry: 3A4A), were obtained from RCSB Protein Data Bank (www.rcsb.org) (Yamamoto et al. 2010). Alpha-D-glucose, calcium ion, and water were removed from the structure, using Visual Molecular Dynamic (VMD) package (Humphrey et al. 1996). Missing polar hydrogens in the structure were added and the atomic charge for all ions was adjusted on the basis of atomic valency. The prepared structure was eventually saved in PDBQT file. All procedures were performed using the Autodock Auxilliary Tool (ADT) version 4.1 (Morris et al. 2009). The 3D-conformers of lupinifolin, 2′′′,3′′′-dihydroxylupinifolin, and genistein were obtained from PubChem with compound CIDs of 5280961, 10250777, and 11048450, respectively. The SDF files were converted to PDB files using Online SMILES translator (https://cactus.nci.nih.gov/translate/). Missing polar hydrogens and charges were optimized using a protocol as a preparation of protein structure. The complete structures were saved in a PDBQT format file. The possible binding mode between α-glucosidase and a compound was analyzed using AutoDock 4.2 (Morris et al. 2009). A grid box of 126 Å x 126 Å x 126 Å with a grid spacing of 0.375 Å was generated in the center of the protein structure using Autogrid program. Docking simulation was performed using the Lamarckian genetic algorithm employed with default parameters. A ligand as a flexible molecule was explored the best position in the grid space of the rigid protein. The docking protocol was consisted of 50

different runs with a population size of 200. After each docking calculation, the best energy conformation of the ligand-protein complex was analyzed.

References

Bakasatae N, Kunworarath N, Yupanqui CT, Voravuthikunchai SP, Joycharat N. 2018. Bioactive components, antioxidant, and anti-inflammatory activities of the wood of *Albizia myriophylla* . Rev Bras Farmacogn. 28:444–450.

Green LC, Wagner DA, Glogowski J, Skipper PL, Wishnok JS, Tannenbaum SR.1982. Analysis of nitrate, nitrite, and [15N] nitrate in biological fluids. Anal Biochem. 126:131–138.

Humphrey W, Dalke A, Schulten K. 1996. VMD: visual molecular dynamics. J Mol Graph. 14:33–38.

Joycharat N, Thammavong S, Limsuwan S, Homlaead S, Voravuthikunchai SP, Yingyongnarongkul B, Dej-adisai S, Subhadhirasakul S. 2013. Antibacterial substances from *Albizia myriophylla* wood against cariogenic *Streptococcus mutans*. Arch Pharm Res. 36:723–730.

Joycharat N, Boonma C, Thammavong S, Yingyongnarongkul B, Limsuwan S, Voravuthikunchai SP. 2016. Chemical constituents and biological activities of *Albizia myriophylla* wood. Pharm Biol. 54:62–73.

Joycharat N, Issarachote P, Sontimuang C, Voravuthikunchai SP. 2018. Alpha-glucosidase inhibitory activity of ethanol extract, fractions and purified compounds from the wood of *Albizia myriophylla*. Nat Prod Res. 32:1291–1294.

Morris GM, Huey R, Lindstrom W, Sanner MF, Belew RK, Goodsell DS, Olson AJ. 2009. AutoDock4 and AutoDockTools4: automated docking with selective receptor flexibility. J Comput Chem. 30:2785–2791.

Yamamoto K, Miyake H, Kusunoki M, Osaki S. 2010. Crystal structures of isomaltase from *Saccharomyces cerevisiae* and in complex with its competitive inhibitor maltose. FEBS J. 277:4205–4214.

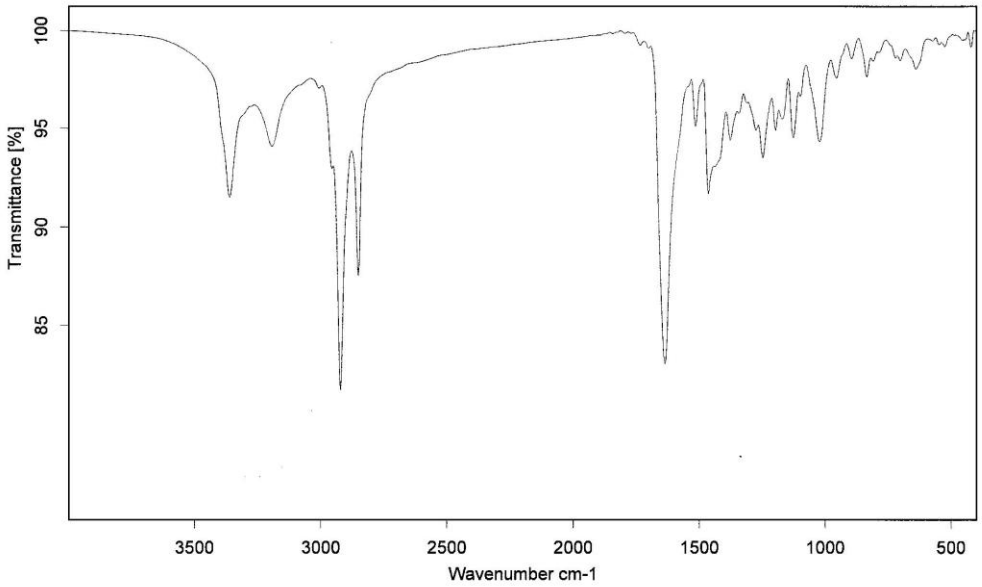

Figure S1. IR spectrum of 4′-methoxydereticulatin (**1**)

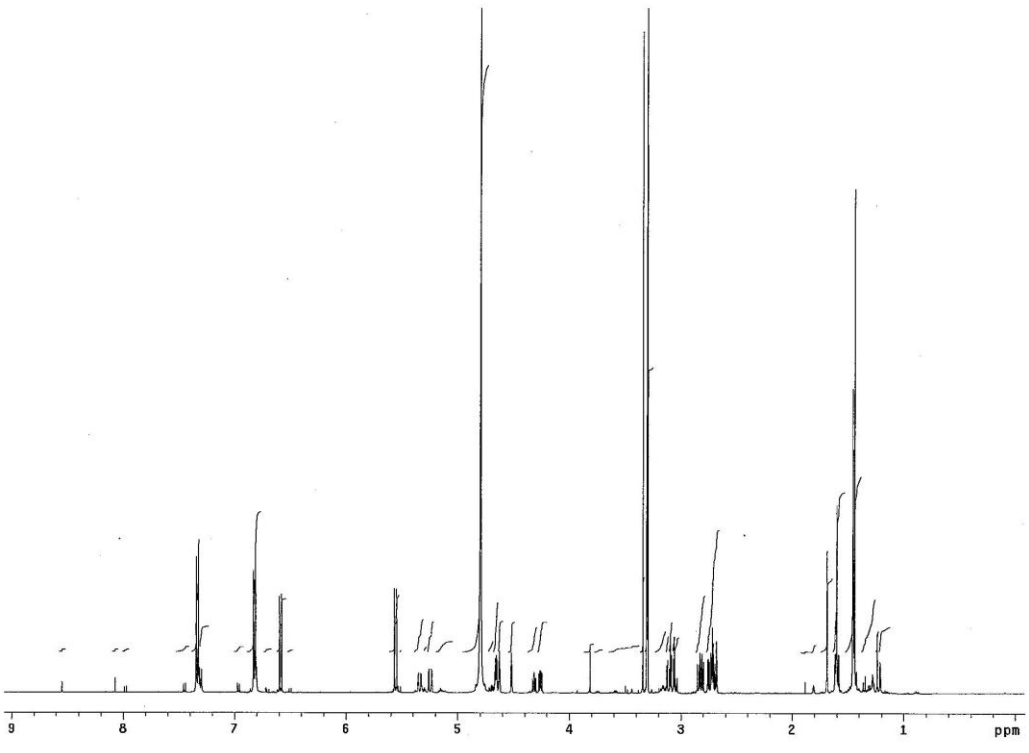

Figure S2. ^{1}H NMR (500 MHz, MeOH-d_4) spectrum of 4′-methoxydereticulatin (**1**)

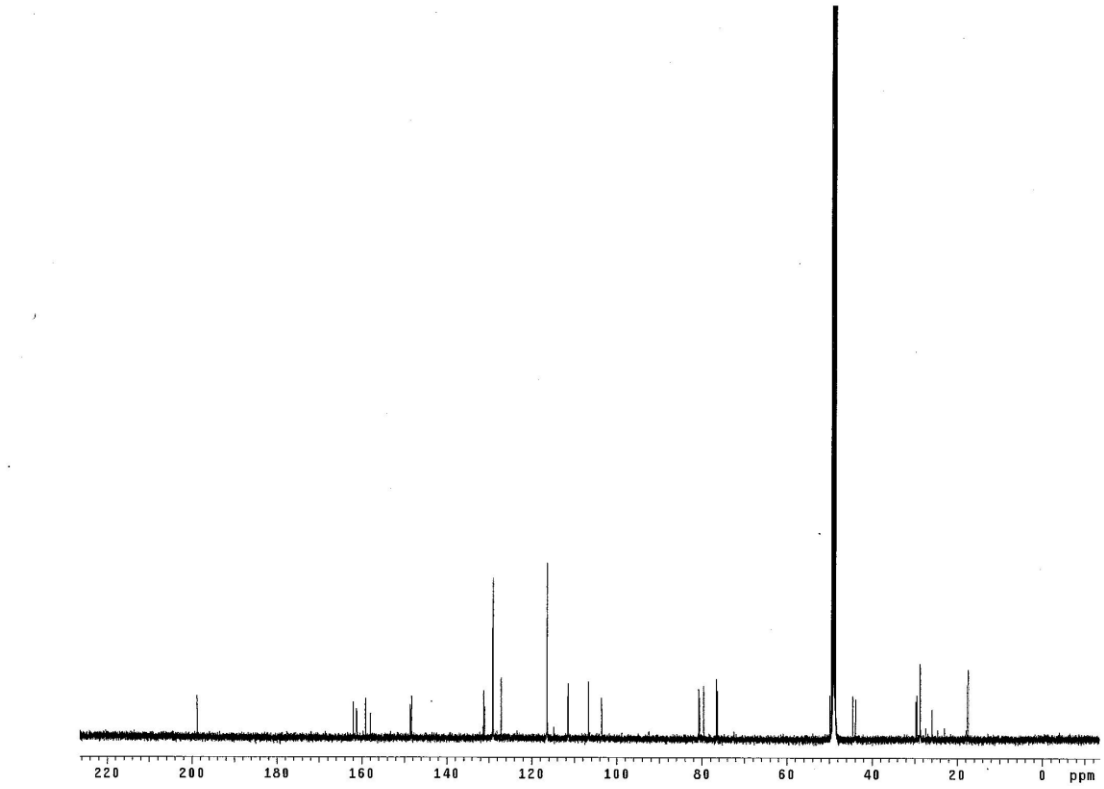

Figure S3. ^{13}C NMR (125 MHz, MeOH-d_4) spectrum of 4′-methoxydereticulatin (**1**)

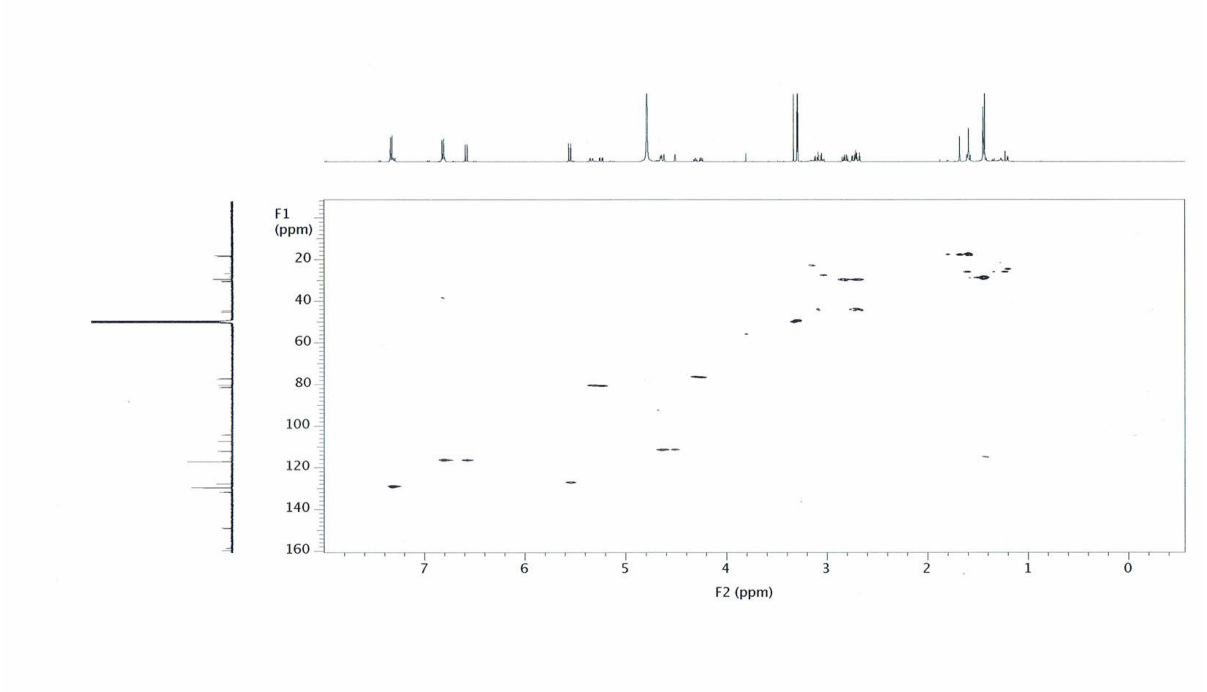

Figure S4. HMQC spectrum of 4′-methoxydereticulatin (**1**)

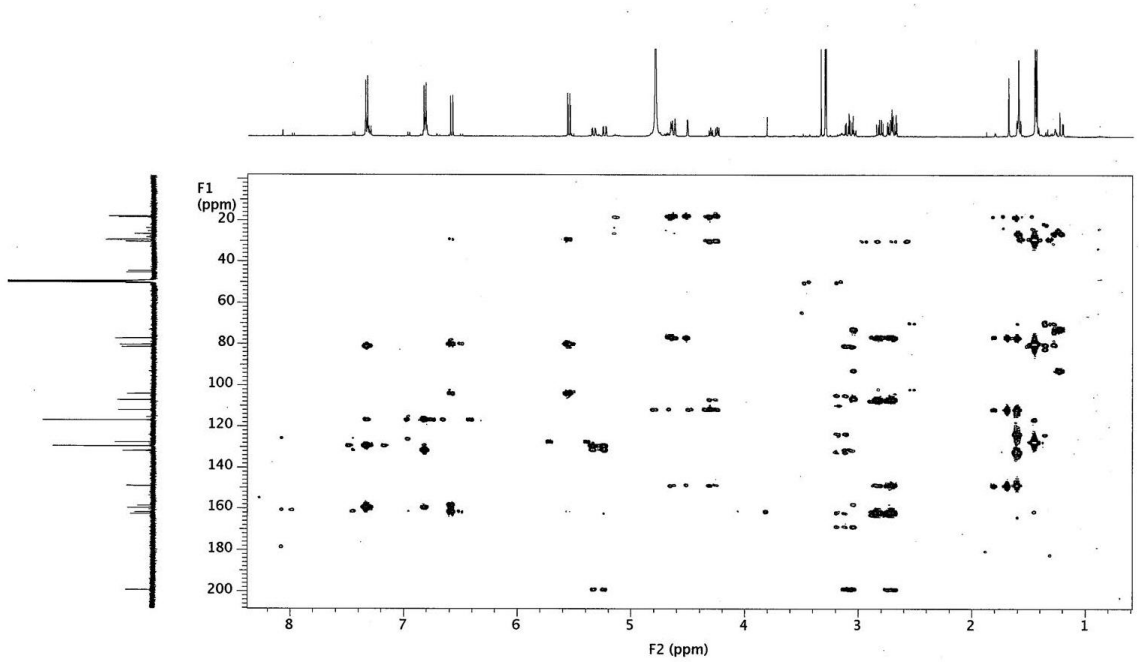

Figure S5. HMBC spectrum of 4′-methoxydereticulatin (**1**)

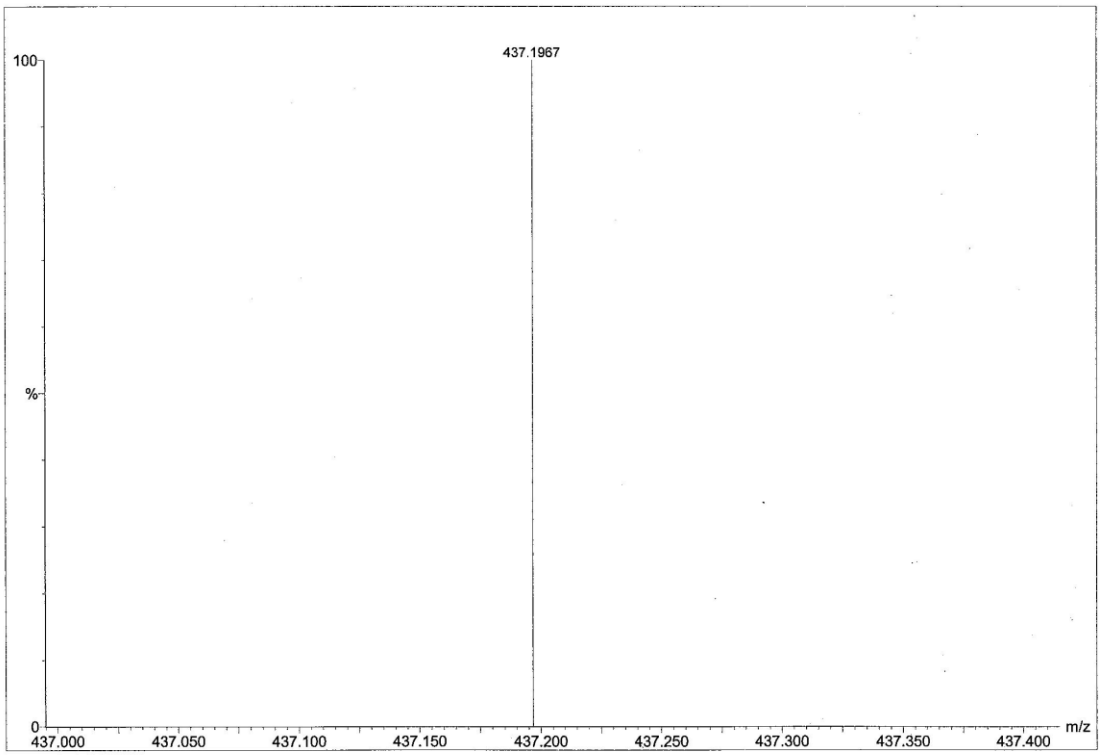

Figure S6. HRESIMS spectrum of 4′-methoxydereticulatin (**1**)

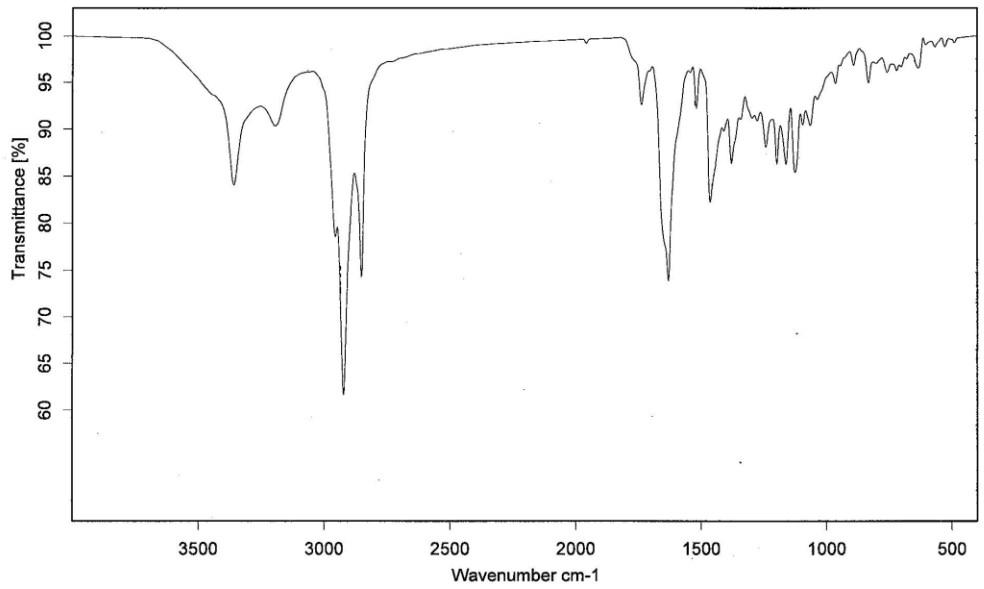

Figure S7. IR spectrum of 2‴-hydroxy,3‴-ethoxylupinifolin (**2**)

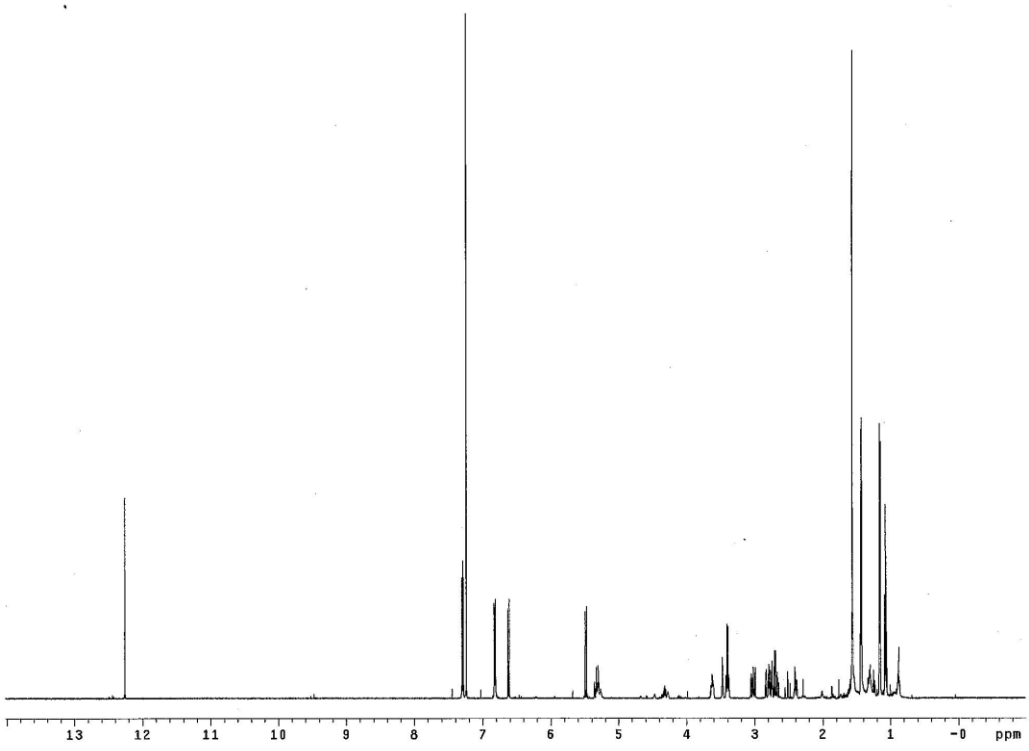

Figure S8. ^{1}H NMR (500 MHz, $CDCl_3$) spectrum of 2‴-hydroxy,3‴-ethoxylupinifolin (**2**)

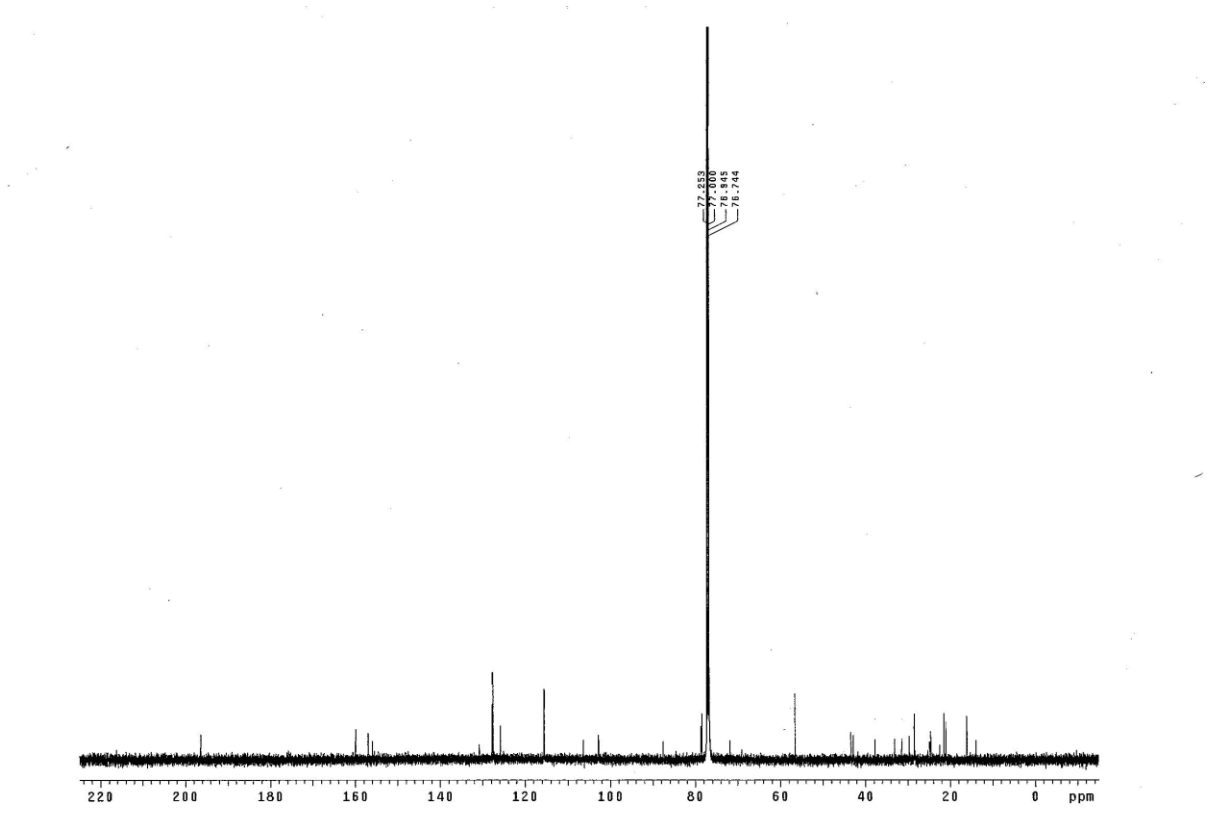

Figure S9. ^{13}C NMR (125 MHz, $CDCl_3$) spectrum of 2‴-hydroxy,3‴-ethoxylupinifolin (**2**)

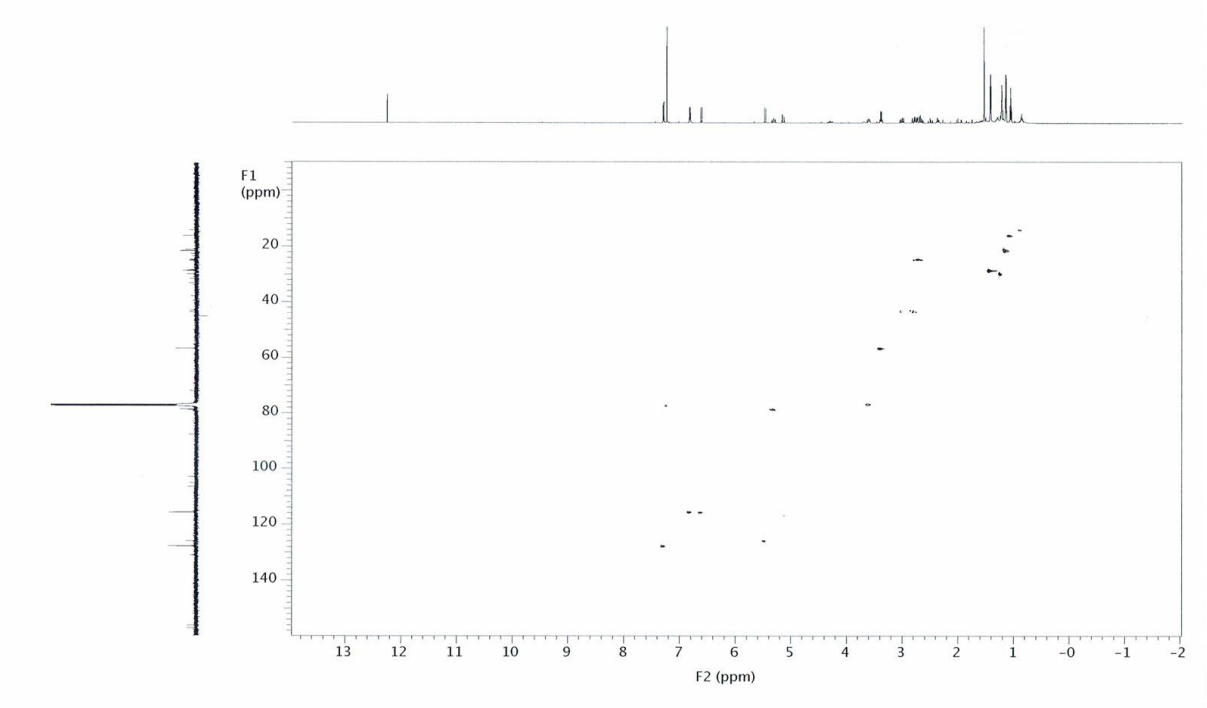

Figure S10. HMQC spectrum of 2‴-hydroxy,3‴-ethoxylupinifolin (**2**)

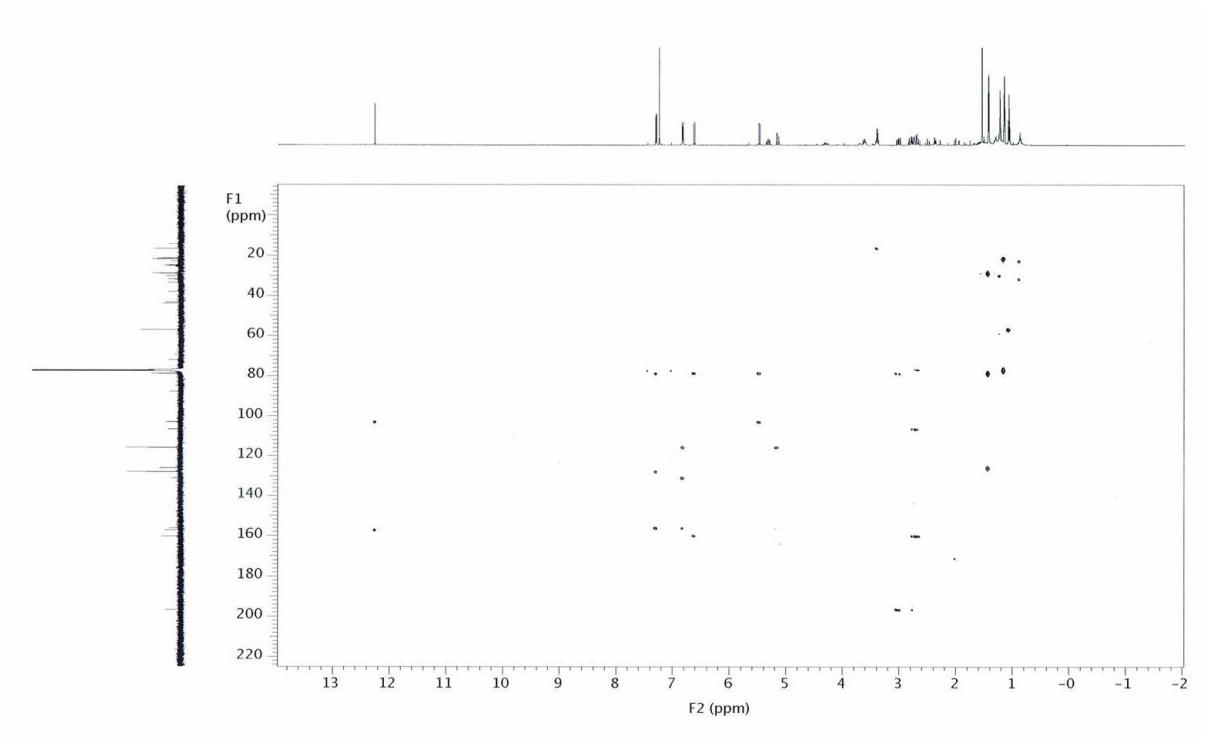

Figure S11. HMBC spectrum of 2‴-hydroxy,3‴-ethoxylupinifolin (**2**)

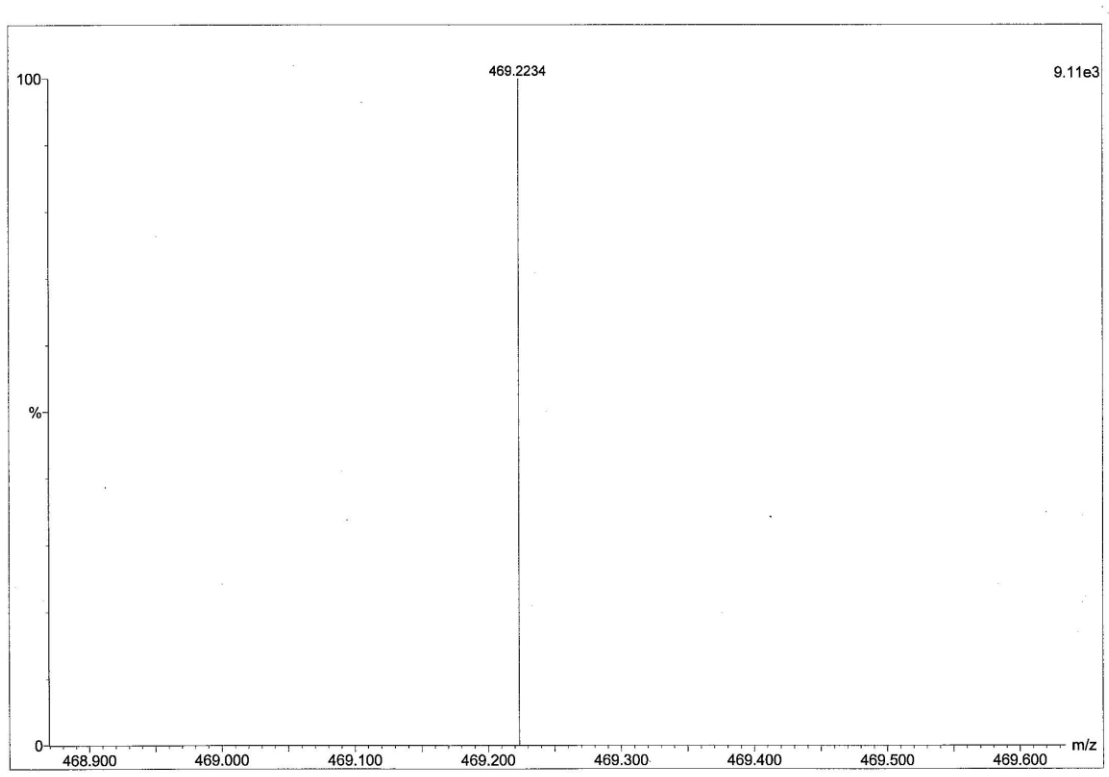

Figure S12. HRESIMS spectrum of 2‴-hydroxy,3‴-ethoxylupinifolin (**2**)

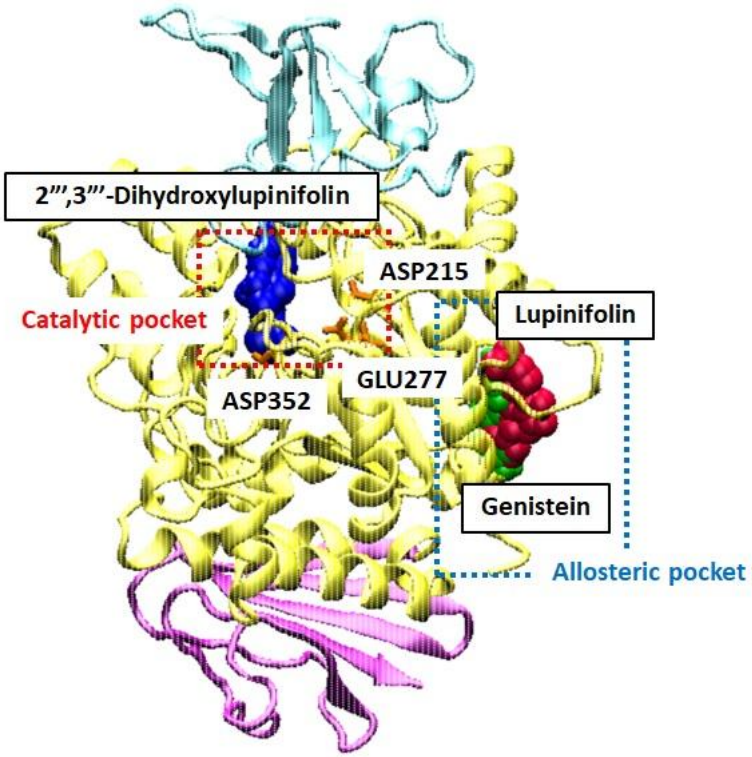

Figure S13. Molecular docking models of α-glucosidase inhibition of genistein (green), lupinifolin (red), and 2′′′,3′′′-dihydroxylupinifolin (blue). α-Glucosidase is composed of three domains; domain A (residues 1–113 and 190–512) in yellow, domain B (residues 114–189) in cyan, and domain C (residues 513–589) in purple. Allosteric and catalytic pocket are indicated by red and blue frames, respectively. The three catalytic residues in the active site pocket including ASP215, ASP352, and GLU277 are shown as an orange licorice model.

Table S1. ^{1}H-NMR, ^{13}C-NMR and HMBC data of 4′-methoxydereticulatin (**1**) in MeOH-d_4

Position	4′-Methoxydereticulatin (**1**)		
	^{1}H (mult, *J* in Hz)	^{13}C	HMBC
2	5.34 (dd, 13, 2.5)	80.79	
3α	3.09 (dd, 17, 13)	44.47	C-2, C-4, C-1′
β	2.82 (dd, 17, 2.5)		
4		198.73	
4a		103.52	
5		159.11	
6		103.55	
7		161.23	
8		106.62	
8a		161.98	
1′		131.22	
2′/6′	7.35 (d, 8)	127.10	C-2, C-1′, C-4′, C-6′/2′
3′/5′	6.91 (d, 8)	116.42	C-1′, C-4′, C-5′/3′
4′		159.11	
1″			
2″		80.79	
3″	5.68 (d, 9.5)	129.10	C-6, C-2″
4″	6.68 (d, 9.5)	116.35	C-5, C-7, C-2″
5″	1.44 (s)	28.62	C-2″, C-3″, C-6″
6″		28.74	C-2″, C-3″, C-5″
1‴α	2.73 (dd, 14, 5)	29.68	C-7, C-8, C-8a, C-2‴
β	3.11 (dd, 14, 8.5)		
2‴	4.25 (dd, 8.5, 5)	76.57	
3‴		148.54	
4‴	4.63 (br s), 4.91 br s)	111.50	C-2‴, C-5‴
5‴	1.60 (s)	17.64	C-2‴, C-3‴, C-4‴
4′-OCH_3	3.33 (s)	49.84	C-4′

Table S2. ^{1}H-NMR, ^{13}C-NMR and HMBC data of 2‴-hydroxy,3‴-ethoxylupinifolin (**2**) in $CDCl_3$

Position	2‴-Hydroxy,3‴-ethoxylupinifolin (**2**)		
	^{1}H (mult, *J* in Hz)	^{13}C	HMBC
2	5.31 (dd, 13.0, 2.5)	78.47	C-2′, C-6′
3α	2.98 (dd, 17.1, 13.0)	43.37	C-2, C-4, C-1′
β	2.72 (dd, 17.1, 2.5)		
4		196.41	
4a		156.95	
5		159.91	
6		102.86	
7		159.96	
8		106.41	
8a		106.37	
1′		130.85	
2′/6′	7.29 (d, 8.5)	127.51	C-2, C-4′, C-6′/2′
3′/5′	6.81 (d, 8.5)	115.58	C-1′, C-4′, C-5′/3′
4′		155.97	
2″		76.74	
3″	5.48 (d, 10.5)	115.51	C-6, C-2″
4″	6.62 (d, 10.5)	125.79	C-5, C-7, C-2″
5″	1.43 (s)	28.56	C-2″, C-3″, C-6″
6″	1.42 (s)	28.46	C-2″, C-3″, C-5″
1‴	2.71, 2.66 (each m)	24.62	C-7, C-8, C-8a
2‴	3.61 (m)	78.69	C-1‴, C4‴/5‴
3‴		87.57	
4‴/5‴	1.14, 1.15 (each s)	21.4	C-2‴
5-OH	12.25		
3‴-OCH_2–CH_3	3.32, 1.07 (each m)	56.56, 16.07	

Table S3. Antibacterial activity of pyranoflavanones **1-4** from *D. reticulata*

Compounds	MIC (μg/mL)				
	S. aureus	*S. epidermidis*	*S. mutans*	*S. sobrinus*	*B. cereus*
1	16	32	32	ND	16
2	ND	ND	> 100	ND	ND
3	12.5	25	0.78	> 100	12.5
4	128	128	64	ND	64
Pen G	0.05	0.05	ND	ND	0.5
Chlorhexidine	ND	ND	0.39	0.39	ND

ND = not determine.

Table S4. Antioxidant activity of some isolates from *D. reticulata*

Compounds	% Radical scavenging (at 250 µg/mL)	
	DPPH	NO
1	41.70	ND
3	14.38	63.60
4	46.42	53.05
5	34.42	38.44
Ascorbic acid	93.80	ND
Catechin	ND	79.51

ND = Not determine.

Table S5. Binding energy (kcal/mol) and inhibitory constant (K_i) of compounds **3-5** with α-glucosidase proteins

Compounds	Molecular formula	Molecular weight (g/mol)	Binding energy (kcal/mol)	Inhibitory constant; K_i (μM)
3	$C_{25}H_{26}O_5$	406.48	-9.34	0.14
4	$C_{25}H_{28}O_7$	440.49	-8.89	0.31
5	$C_{15}H_{10}O_5$	270.24	-7.83	1.83